

FILE COPY
NO. 7

CASE FILE COPY

NATIONAL ADVISORY COMMITTEE FOR AERONAUTICS

REPORT No. 515

FULL-SCALE WIND-TUNNEL TESTS OF A PCA-2 AUTOGIRO ROTOR

By JOHN B. WHEATLEY and MANLEY J. HOOD



NACA FILE COPY

Loan expires on last
date stamped on back cover.

PLEASE RETURN TO

REPORT DISTRIBUTION AND STORAGE SECTION
LANGLEY AERONAUTICAL LABORATORY
NATIONAL ADVISORY COMMITTEE
FOR AERONAUTICS

Langley Field, Virginia

1935

AERONAUTIC SYMBOLS I. FUNDAMENTAL AND DERIVED UNITS

Symbol	Metric		English	
	Unit	Abbreviation	Unit	Abbreviation
Length	meter	m	foot (or mile)	ft. (or mi.)
Time	second	s	second (or hour)	sec. (or hr.)
Force	weight of 1 kilogram	kg.	weight of 1 pound	lb.
Power	horsepower (metric)		horsepower	hp.
Speed	kilometers per hour meters per second	k.p.h. m.p.s.	miles per hour feet per second	m.p.h. f.p.s.

2. GENERAL SYMBOLS

- W , Weight = mg
 a , Standard acceleration of gravity = 9.80665 m/s² or 32.1740 ft./sec.²
 m , Mass = $\frac{W}{g}$
 L , Moment of inertia = mk^2 (Indicate axis of radius of gyration k by proper subscript.)
 μ , Coefficient of viscosity

3. AERODYNAMIC SYMBOLS

- S , Area
 S_w , Area of wing
 c , Gap
 b , Span
 c , Chord
 λ , Aspect ratio
 V , True air speed
 q , Dynamic pressure = $\frac{1}{2}\rho V^2$
 L , Lift, absolute coefficient $C_L = \frac{L}{qS}$
 D , Drag, absolute coefficient $C_D = \frac{D}{qS}$
 D_p , Profile drag, absolute coefficient $C_{D_p} = \frac{D_p}{qS}$
 D_i , Induced drag, absolute coefficient $C_{D_i} = \frac{D_i}{qS}$
 D_p , Parasite drag, absolute coefficient $C_{D_p} = \frac{D_p}{qS}$
 C , Cross-wind force, absolute coefficient $C_C = \frac{C}{qS}$
 R , Resultant force
- ν , Kinematic viscosity
 ρ , Density (mass per unit volume)
 Standard density of dry air, 0.12497 kg-m⁻³ at 15° C. and 760 mm., or 0.002378 lb.-ft.⁻³ sec.
 Specific weight of "standard" air, 1.2255 kg/m³ or 0.07651 lb./cu.ft.
- α , Angle of setting of wings (relative to thrust line)
 α_s , Angle of stabilizer setting (relative to thrust line)
 Q , Resultant moment
 Ω , Resultant angular velocity
 $\frac{V}{\rho L}$, Reynolds Number, where L is a linear dimension (e.g., for a model airfoil 3 in. chord, 100 m.p.h. normal pressure at 15° C., the corresponding number is 234,000; or for a model of 10 cm. chord, 40 m.p.s. the corresponding number is 274,000)
 C_p , Center-of-pressure coefficient (ratio of distance of C_p from leading edge to chord length)
 α , Angle of attack
 ϵ , Angle of downwash
 α_0 , Angle of attack, infinite aspect ratio
 α_i , Angle of attack, induced
 α_a , Angle of attack, absolute (measured from zero-lift position)
 γ , Flight-path angle

REPORT No. 515

**FULL-SCALE WIND-TUNNEL TESTS OF A
PCA-2 AUTOGIRO ROTOR**

By JOHN B. WHEATLEY and MANLEY J. HOOD
Langley Memorial Aeronautical Laboratory

NATIONAL ADVISORY COMMITTEE FOR AERONAUTICS

HEADQUARTERS, NAVY BUILDING, WASHINGTON, D.C.

LABORATORIES, LANGLEY FIELD, VA.

Created by act of Congress approved March 3, 1915, for the supervision and direction of the scientific study of the problems of flight. Its membership was increased to 15 by act approved March 2, 1929. The members are appointed by the President, and serve as such without compensation.

JOSEPH S. AMES, Ph.D., *Chairman*,

President, Johns Hopkins University, Baltimore, Md.

DAVID W. TAYLOR, D.Eng., *Vice Chairman*,

Washington, D.C.

CHARLES G. ABBOT, Sc.D.,

Secretary, Smithsonian Institution.

LYMAN J. BRIGGS, Ph.D.,

Director, National Bureau of Standards.

BENJAMIN D. FOULDS, Major General, United States Army,

Chief of Air Corps, War Department.

HARRY F. GUGGENHEIM, M.A.,

Port Washington, Long Island, N.Y.

ERNEST J. KING, Rear Admiral, United States Navy,

Chief, Bureau of Aeronautics, Navy Department.

CHARLES A. LINDBERGH, LL.D.,

New York City.

WILLIAM P. MACCRACKEN, Jr., Ph.B.,

Washington, D.C.

CHARLES F. MARVIN, Sc.D.,

United States Weather Bureau.

HENRY C. PRATT, Brigadier General, United States Army,

Chief, Matériel Division, Air Corps, Wright Field, Dayton, Ohio.

EUGENE L. VIDAL, C.E.,

Director of Aeronautics, Department of Commerce.

EDWARD P. WARNER, M.S.,

Editor of Aviation, New York City.

R. D. WEYERBACHER, Commander, United States Navy,

Bureau of Aeronautics, Navy Department.

ORVILLE WRIGHT, Sc.D.,

Dayton, Ohio.

GEORGE W. LEWIS, *Director of Aeronautical Research*

JOHN F. VICTORY, *Secretary*

HENRY J. E. REID, *Engineer in Charge, Langley Memorial Aeronautical Laboratory, Langley Field, Va.*

JOHN J. IDE, *Technical Assistant in Europe, Paris, France*

TECHNICAL COMMITTEES

AERODYNAMICS
POWER PLANTS FOR AIRCRAFT
MATERIALS FOR AIRCRAFT

Coordination of Research Needs of Military and Civil Aviation

Preparation of Research Programs

Allocation of Problems

Prevention of Duplication

Consideration of Inventions

PROBLEMS OF AIR NAVIGATION
AIRCRAFT ACCIDENTS
INVENTIONS AND DESIGNS

LANGLEY MEMORIAL AERONAUTICAL LABORATORY

LANGLEY FIELD, VA.

Unified conduct for all agencies of scientific research on the fundamental problems of flight.

OFFICE OF AERONAUTICAL INTELLIGENCE

WASHINGTON, D.C.

Collection, classification, compilation, and dissemination of scientific and technical information on aeronautics.

REPORT No. 515

FULL-SCALE WIND-TUNNEL TESTS OF A PCA-2 AUTOGIRO ROTOR

By JOHN B. WHEATLEY and MANLEY J. HOOD

SUMMARY

This paper presents the results of force tests on and air-flow surveys near a PCA-2 autogiro rotor in the N. A. C. A. full-scale wind tunnel. The force tests were made at three pitch settings and several rotor speeds; the effect of fairing protuberances on the rotor blade was determined. Induced downwash and yaw angles were determined at two tip-speed ratios in a plane 1½ feet above the path of the blade tips. The results show that the maximum L/D of the rotor cannot be appreciably increased by increasing the blade pitch angle above about 4.5° at the blade tip; that the protuberances on the blades cause more than 5 percent of the total rotor drag; and that the rotor center-of-pressure travel is very small.

INTRODUCTION

The National Advisory Committee for Aeronautics has for several years been making an intensive study of rotating-wing aircraft initiated because of the definite promise of this type of flying machine in the related fields of safety and low-speed control. The experimental work completed to date has consisted of flight tests on a PCA-2 autogiro (references 1 and 2) from which the gliding performance, fixed-wing loads, and rotor-blade motion of the machine were determined. Following these tests an attempt was made to deduce from them the aerodynamic characteristics of the rotor (reference 3), but the results were unsatisfactory for several reasons. No quantitative evaluation of the interference of the remainder of the machine upon the rotor was possible, but the most serious fault with the results lay in the fact that the drag of the rotor, its most important characteristic, could not be found. In order to obtain complete and accurate information concerning the aerodynamic characteristics of the PCA-2 autogiro rotor and to supply data applicable to an analysis of the sources of its drag, the rotor was removed from the machine and tested alone in the full-scale wind tunnel at Langley Field in December 1933.

The test program included force tests at one pitch setting and several rotor speeds with the blade protuberances both exposed and faired, and at two

additional pitch settings and at several rotor speeds with the protuberances faired. In addition, air-flow surveys were made at two air speeds in a plane parallel to and about 1½ feet above the path described by the blade tips.

This report contains a presentation of the data obtained in the full-scale wind-tunnel tests. The results of an analysis of this information will be subsequently published.

APPARATUS

The autogiro rotor used in these tests is shown mounted in the wind tunnel in figure 1; figure 2 shows its geometrical characteristics. For the first tests the rotor was exactly as furnished on the PCA-2 autogiro (fig. 3 (a)), but during all subsequent tests there were fairings over the droop-cable fittings and damping devices for the interblade cables (fig. 3 (b)).

The N. A. C. A. full-scale wind tunnel, together with its 6-component balance and air-flow survey apparatus used for these tests, is described in detail in reference 4. Sphere drag tests made since this reference was published show the critical Reynolds Number in the wind tunnel to be between 340,000 and 370,000, indicating the turbulence, as measured by this method, to be about the same as has been found in free air. (See reference 5.)

The rotor was supported on the balance by a steel tube tripod having an apex formed by a steel casting containing a mechanism for changing the angle of attack. This mechanism consisted of a double worm and gear reduction operated by a hand crank in the balance house. The angle of attack (the acute angle between the direction of flight and a plane perpendicular to the rotor axis) was indicated by a revolution counter geared to the crank shaft. The entire supporting system beneath the rotor was shielded from the air stream to eliminate tare drag.

The rotor speed was obtained from an indicator at the angle-of-attack control station, connected to a tachometer magneto driven by the rotor. An additional indicator was placed at the wind-tunnel control station for the use of the tunnel operator while the rotor was being started.

TEST PROCEDURE

The rotor was started by the air stream, no mechanical starting gear having been incorporated in the test set-up. The rotor was set at about 10° angle of at-

necessary readings were taken. The angle of attack was then adjusted to give other desired rotor speeds, readings were again taken, and the process was repeated at other air speeds. For each condition of

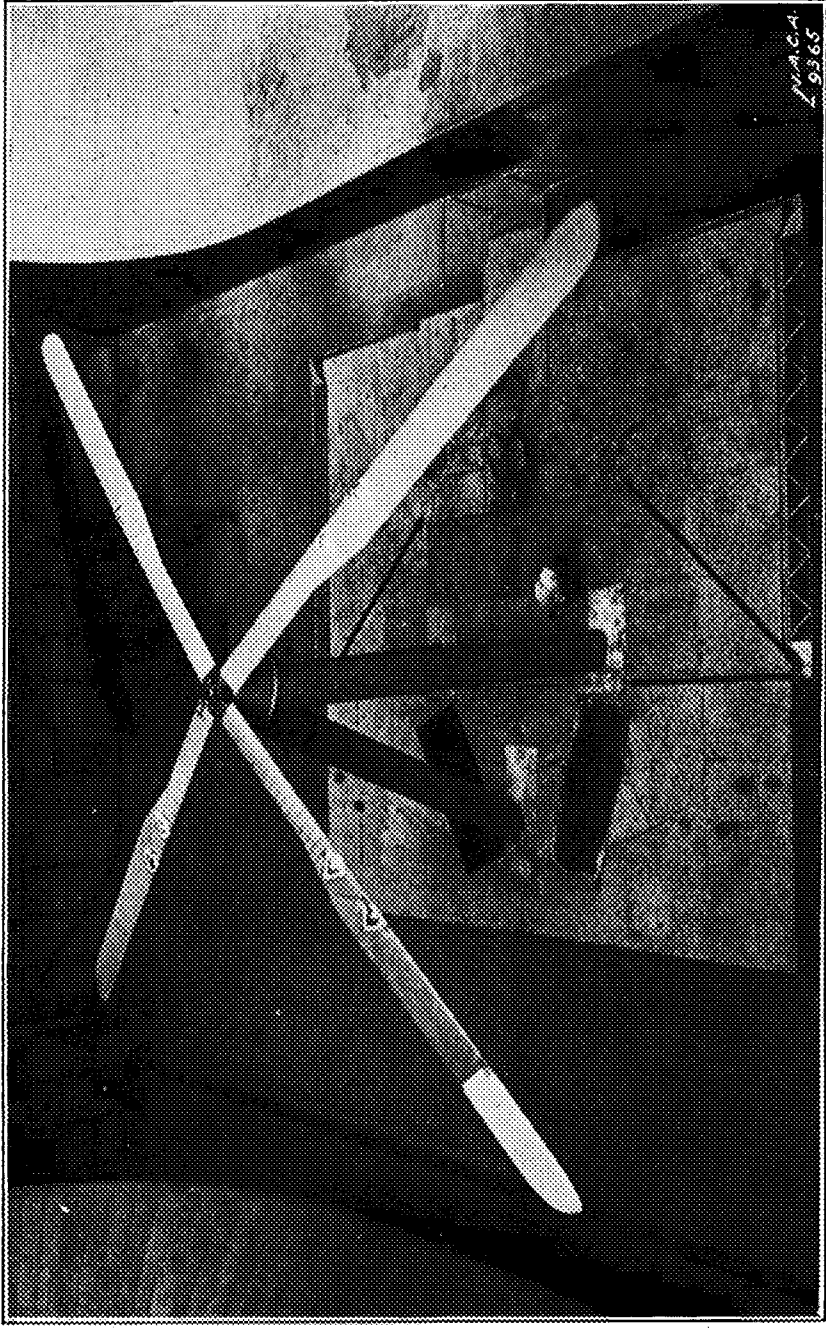


FIGURE 1.—PCA-2 autogiro rotor in N. A. C. A. full-scale wind tunnel.

tack, the wind tunnel was started slowly by jogging on and off the lowest-speed switch point, and the air speed was gradually increased as the rotor picked up speed.

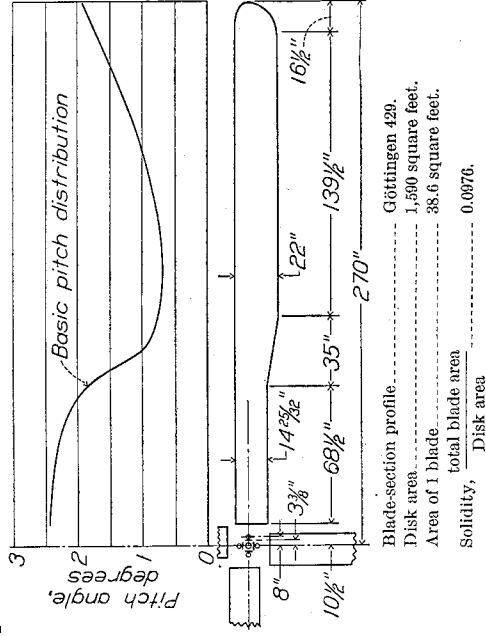
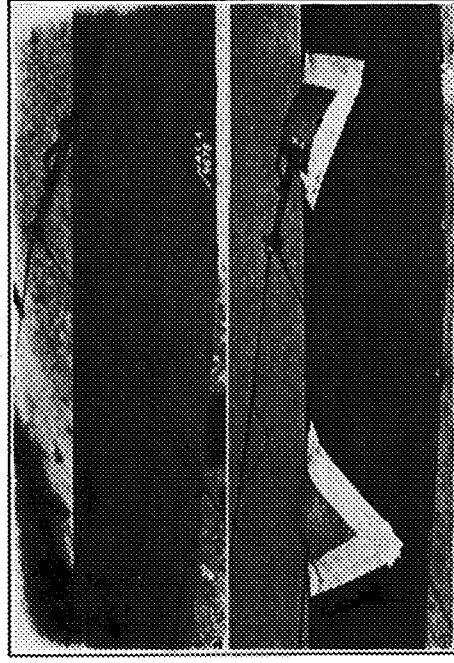


FIGURE 2.—Geometrical characteristics of the PCA-2 autogiro rotor.

Force tests were made by the following procedure: The wind-tunnel control was set for the lowest air speed, the angle of attack was adjusted so the rotor operated steadily at a desired rotor speed, and the

operation the readings of all the scales were mechanically recorded and visual readings were taken of rotor speed, rotor angle of attack, and air-stream dynamic



(a) Protuberances exposed.
(b) Protuberances faired.

FIGURE 3.—Protuberances on PCA-2 autogiro rotor blade.

pressure. In order to compute true air speed, the air temperature, barometric pressure, and wet- and dry-bulb temperatures were obtained by visual observations at intervals during the test.

The highest angle of attack at which it was possible to test the rotor in the wind tunnel was limited in some cases by the fact that the tunnel cannot be operated below 23 miles per hour and in other cases by the jet size. At the highest angle of attack (26° uncorrected), the blade tips were 3.6 feet and 5.9 feet from the top and bottom boundaries of the jet, respectively. The lowest angle of attack at which the rotor could be tested was limited by the highest air speed available, 119 miles per hour, with the rotor in the jet.

Air-flow surveys were made in a plane approximately parallel to and about $1\frac{1}{2}$ feet above the circle described by the blade tips. The apparatus and method used are described in reference 4, except that angles were measured by the pressure method instead of by the null, or alinement, method.

When the pitch setting of the rotor blades was changed it was adjusted within 0.1° with a level protractor. In order to check the track of the blades, the rotor was run and a paint brush was lowered onto the rotor from above until the high blades were marked. Indicated adjustments were then made and the process repeated until the rotor operated smoothly as indicated by the steadiness of the balance scales. When the rotor operation was considered satisfactory, the blade tips tracked to within about $1\frac{1}{2}$ inches.

RESULTS

The results of the tests are contained in tables I to IV and figures 4 to 17, inclusive. All data have been corrected for jet-boundary and blocking effect; in addition, the drag of the rotor hub was measured

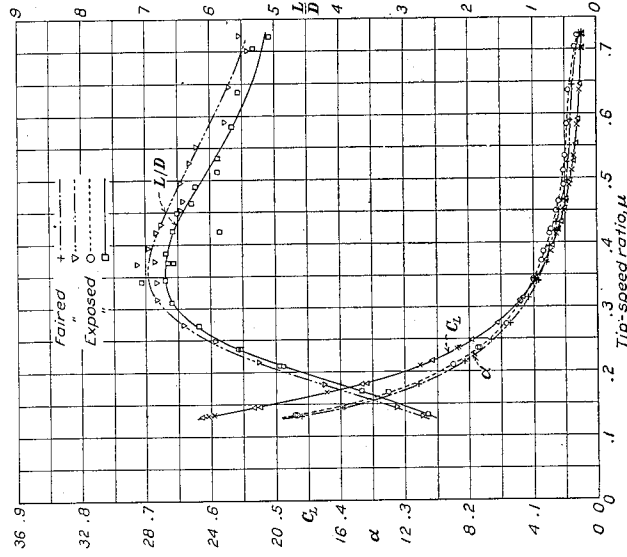


FIGURE 4.—PCA-2 autogiro rotor characteristics, $\theta=3.0^\circ$, pitch setting = 1.9° , $N=100$ r. p. m., protuberances faired and exposed.

with the blades removed and subtracted from the rotor drag.

It will be noted that the nominal pitch angle, represented by the symbol θ , differs from the pitch setting

noted on each figure and is not constant at a given pitch setting. The nominal pitch angle is the pitch

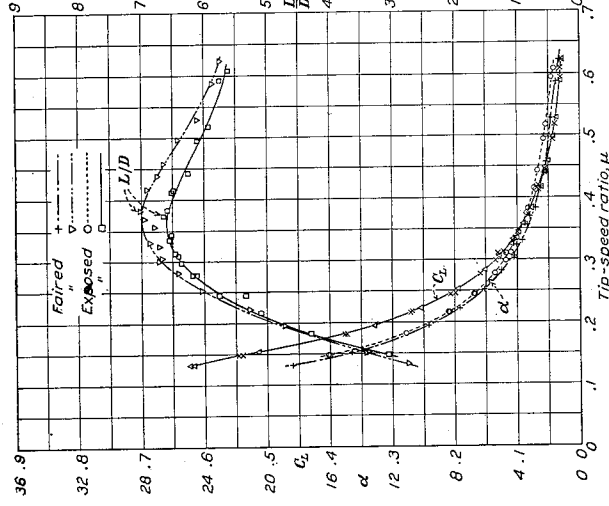


FIGURE 5.—PCA-2 autogiro rotor characteristics, $\theta=3.2^\circ$, pitch setting = 1.9° , $N=120$ r. p. m., protuberances faired and exposed.

angle of the tip of the rotor blade under operating conditions and the pitch setting is the pitch angle at

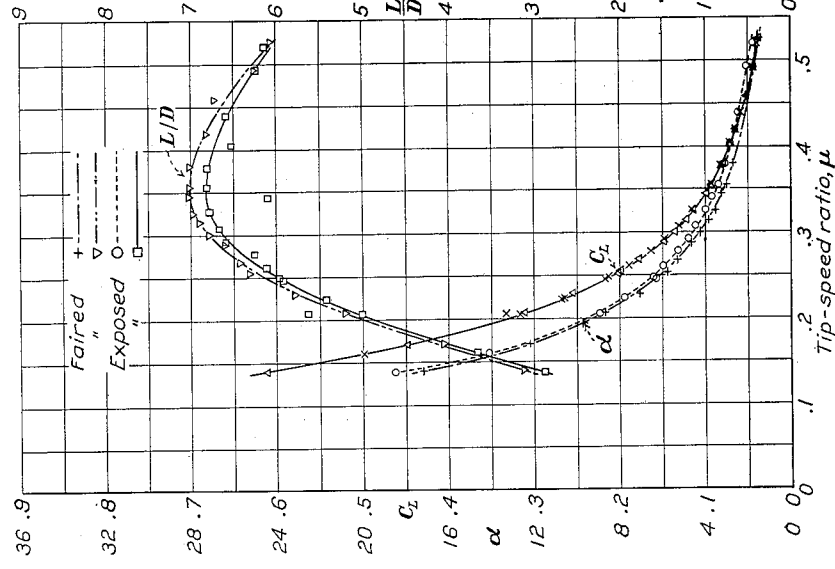


FIGURE 6.—PCA-2 autogiro rotor characteristics, $\theta=3.7^\circ$, pitch setting = 1.9° , $N=140$ r. p. m., protuberances faired and exposed.

the tip of the rotor blade when at rest. The difference between the two is the dynamic twist, arising because the component of centrifugal force normal to the rotor blade is applied aft of the blade center of pressure;

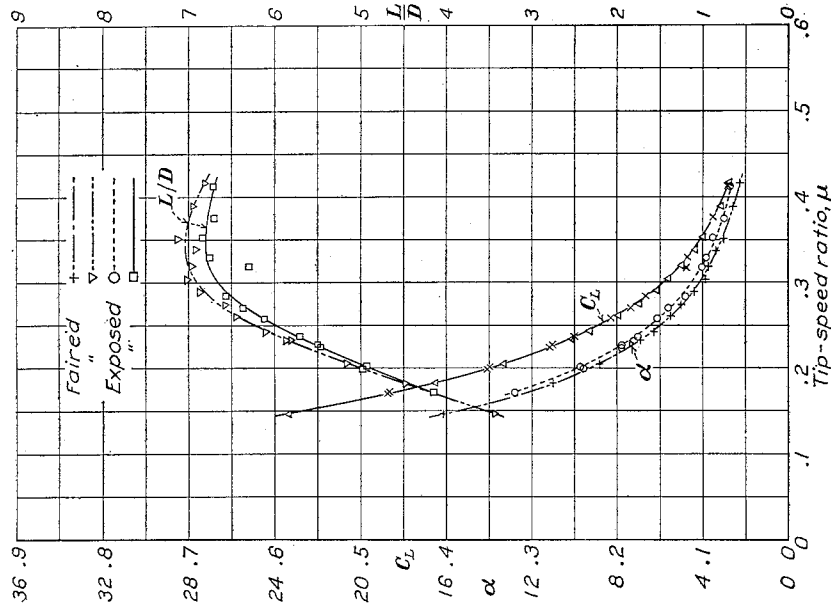


FIGURE 7.—PCA-2 autogiro rotor characteristics, $\theta = 4.0^\circ$, pitch setting = 1.9° , $N = 150$ r. p. m., protuberances faired and exposed.

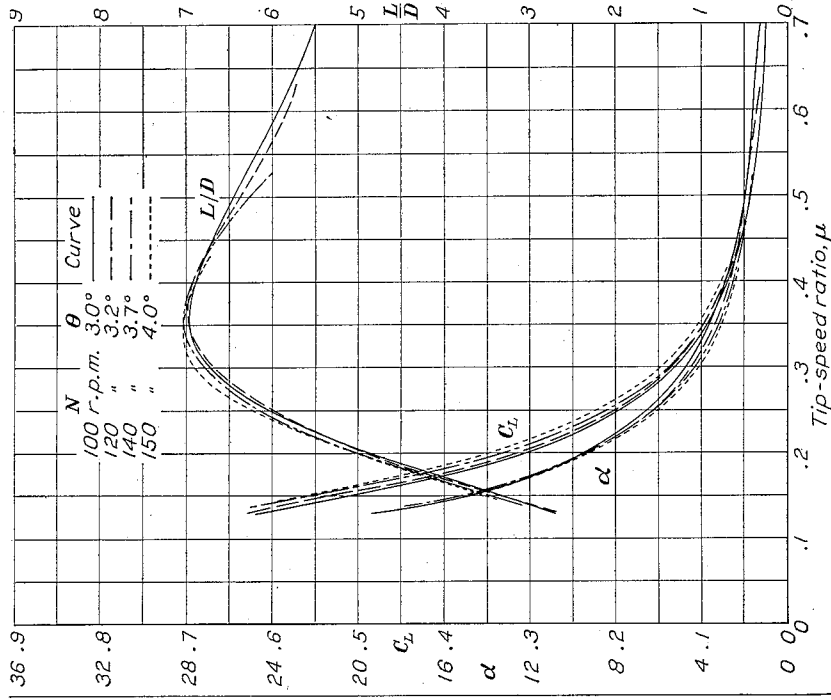


FIGURE 9.—PCA-2 autogiro rotor characteristics with protuberances faired, pitch setting = 1.9° .

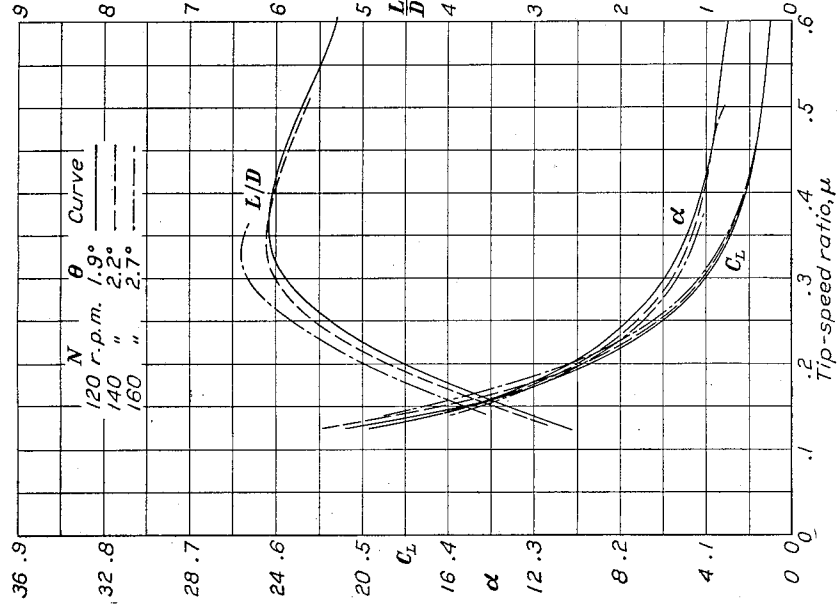


FIGURE 8.—PCA-2 autogiro rotor characteristics with protuberances faired, pitch setting = 0.8° .

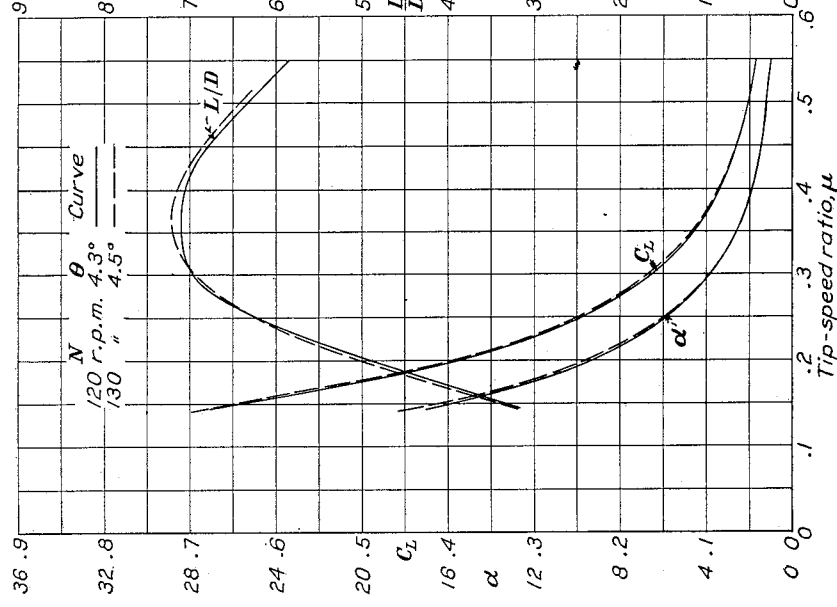


FIGURE 10.—PCA-2 autogiro rotor characteristics with protuberances faired, pitch setting = 2.7° .

the couple resulting from these two forces is within small limits proportional to the thrust, so the dynamic twist also varies with the thrust. Flight tests on the PCA-2 rotor established the fact that the dynamic twist is about 0.89° at the tip for 1,000 pounds thrust, and the nominal pitches assigned to the different runs made in the wind-tunnel tests were determined from this relation, employing the average thrust obtained at a given rotor speed.

Figures 4 to 7 show the influence on the L/D and angle of attack of the rotor resulting from fairing the blade protuberances shown in figure 3, the results being presented for one pitch setting and for several rotor speeds. Figures 8 to 10 show the influence of a change in the pitch setting of the rotor, curves being shown on each figure for different designated rotor speeds. Experimental points have been omitted on figures 8 to 10 because the curves are so close together that confusion would have resulted had they been included. The quantity and dispersion of the test points are, however, the same for these figures as for figures 4 to 7.

In figures 11 to 13 are presented vector sheaves for the three pitch settings tested. The accidental errors

in the measurements of aerodynamic moments were as large as or larger than the differences caused by varying the rotor speed. For this reason, the average value of the moment coefficients obtained at different rotor speeds was used to construct the vector maps of the

Figures 14 and 15 contain the contour maps of the downwash angles measured in a plane about $1\frac{1}{2}$ feet above the tips of the rotor blades, and figures 16 and 17 show the contour maps of the yaw angles measured in the same plane.

PRECISION

The relation between blade pitch angle and rotor thrust that was used in assigning values of nominal pitch angle to the various curves presented herein was established by photographic studies of the rotor in flight. The precision of the results so obtained was sufficient to determine the proportionality between the thrust and dynamic twist to within about 10 percent, and the nominal pitch is considered accurate to within $\pm 0.2^\circ$.

The accidental errors disclosed by the dispersion of the experimental points in figures 4 to 7 may be

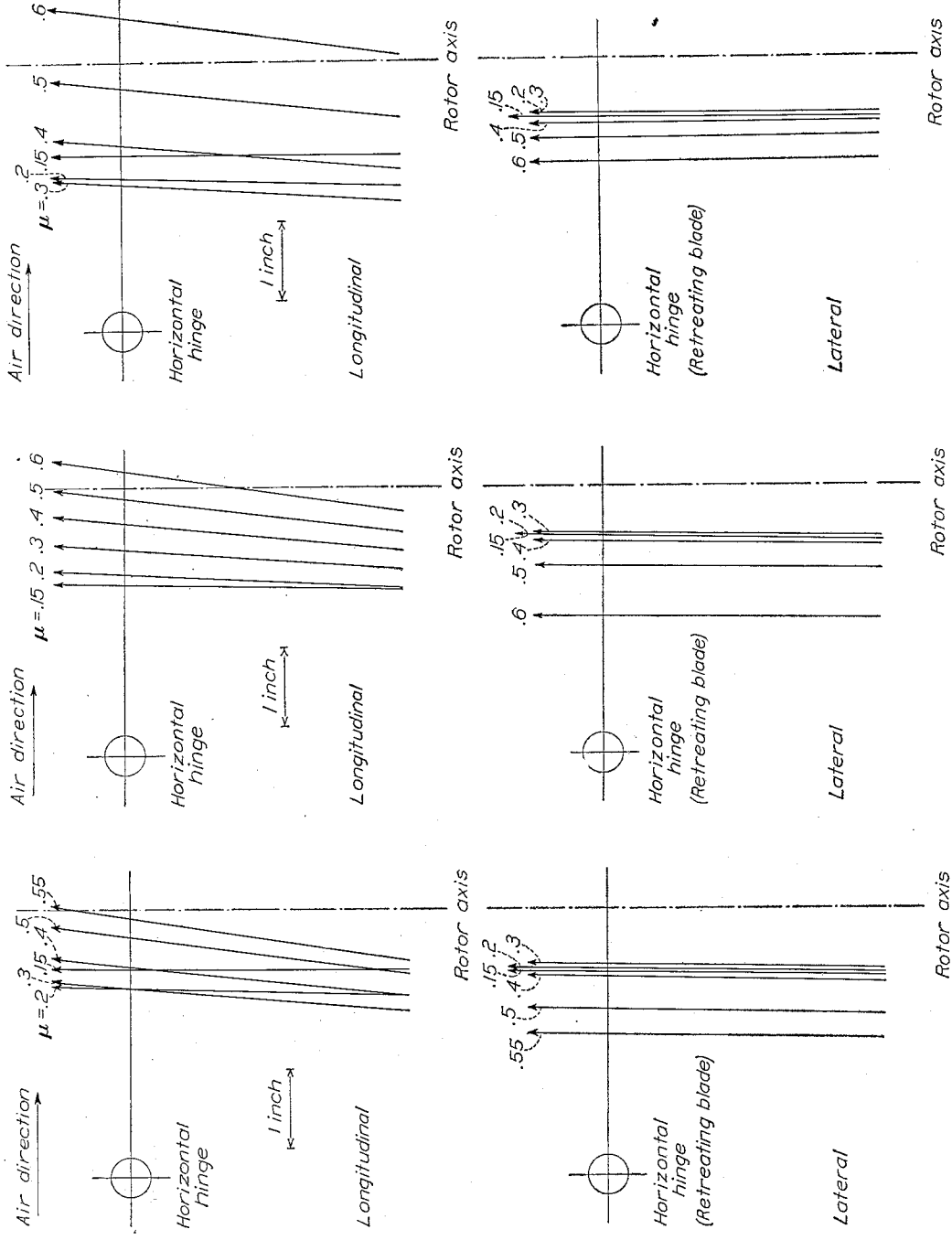


FIGURE 11.—Vector sheaf of PCA-2 autogiro rotor, pitch setting = 0.8° .

FIGURE 12.—Vector sheaf of PCA-2 autogiro rotor, pitch setting = 1.9° .

FIGURE 13.—Vector sheaf of PCA-2 autogiro rotor, pitch setting = 2.7° .

ascribed to the following possible causes: Failure to obtain steady conditions on the rotor before taking readings, fluctuations in the dynamic pressure and rotor speed as readings were taken, and observational

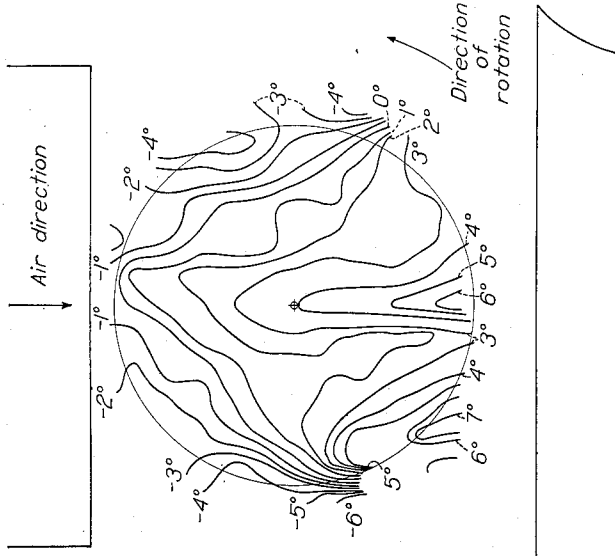


FIGURE 14.—Downwash angle distribution over disk of PCA-2 autogiro rotor, $\mu=0.294$, $N=120$ r. p. m., pitch setting=1.9°.

errors in reading the dynamic pressure and rotor speed. The number of experimental points is, however, sufficient to reduce the accidental error in the faired curves of the figures to a negligible value.

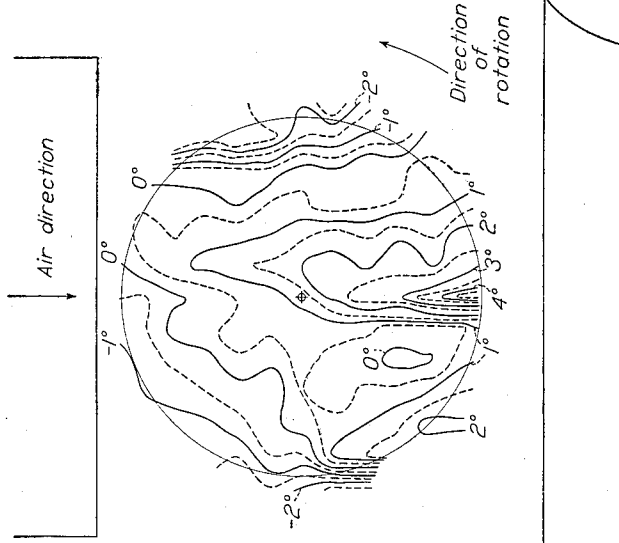


FIGURE 15.—Downwash angle distribution over disk of PCA-2 autogiro rotor, $\mu=0.448$, $N=115$ r. p. m., pitch setting=1.9°.

Consistent errors in the results may be considered as arising only from the blocking and jet-boundary corrections applied to the measured coefficients. These forces were so small a percentage of measured forces that they may be neglected in this consideration. The

blocking correction, necessitated by the disturbance of the uniform velocity distribution across the jet by a body in the jet, was determined by velocity surveys across the wind-tunnel return passage accurately

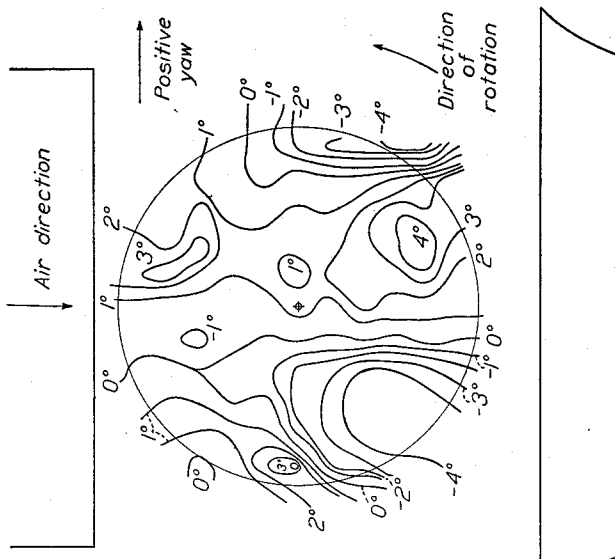


FIGURE 16.—Induced yaw distribution over disk of PCA-2 autogiro rotor, $\mu=0.294$, $N=120$ r. p. m., pitch setting=1.9°.

enough to insure dynamic pressure being correct within ± 1 percent. The jet-boundary correction was applied as in reference 6, the value of the correction factor δ being assumed equal to that for an airfoil of

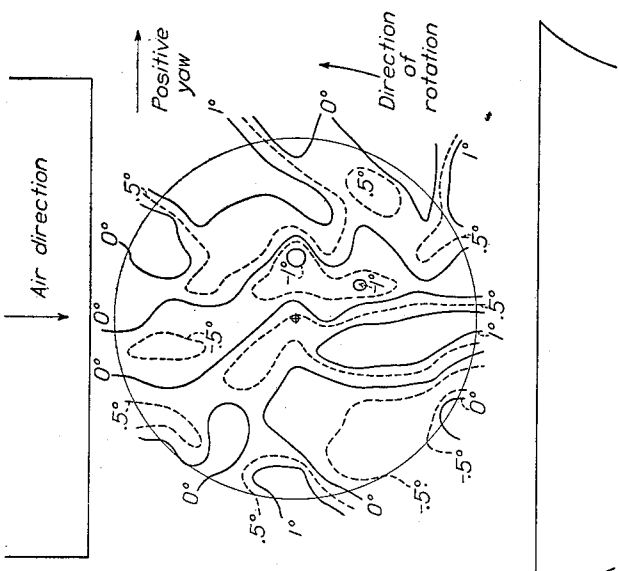


FIGURE 17.—Induced yaw distribution over disk of PCA-2 autogiro rotor, $\mu=0.448$, $N=115$ r. p. m., pitch setting=1.9°.

span equal to the rotor diameter. It is recognized that the trailing vortices behind the rotor are in all probability essentially different in distribution from those behind a wing, but this discrepancy may be corrected by using a slightly different equivalent span for

the rotor. The value of δ is, however, almost constant for all wing spans between 35 and 45 feet and, since the rotor diameter is 45 feet, this value of the span was used to determine δ .

Unfortunately, no quantitative value could be assigned to the correction that should be applied to the measured downwash angles at different stations along the chord of the rotor disk. Studies of this question, soon to be published, indicated that in this case the correction would be less than 10 percent of the measured value of the downwash angle at the trailing edge of the disk, or less than 1°, and the correction would be zero near the transverse diameter of the disk. Because quantitative information was lacking, no correction was made to the survey results except the subtraction of a constant value equal to the jet-boundary effect on angle of attack. The contours shown are thought to be within 1 foot of their correct position.

The vector sheaves shown in figures 11 to 13 include errors in both the moment and lift coefficients. The relative magnitudes of the coefficients and the number of experimental points are such, however, that the position of each vector is determined to within $\pm \frac{1}{4}$ inch.

The following table summarizes the precision of the results arrived at from the previous discussion:

C_L	± 2 percent.
L/D	± 4 percent.
C_T	± 8 percent.
α	$\pm 0.2^\circ$.
μ	± 2 percent.
N	± 0.5 percent.
C_l	± 20 percent.
C_m	± 20 percent.
Vectors.....	$\pm \frac{1}{4}$ inch.
Contours.....	± 1 foot.

DISCUSSION

Change of nominal pitch angle with thrust.—The importance of assigning the correct nominal pitch angle to each run made in the tunnel tests lies in the sensitivity of the fundamental parameters of the rotor to small changes in pitch. The data obtained in these tests were intended primarily for analytical purposes and, for this reason, every effort was made in preliminary flight tests to establish definitely the relations governing the changes in pitch with the rotor operating conditions. It is thought that the accurate determination of the pitch angle eliminates a major source of discrepancies in the data which otherwise might occur during analysis.

Effect of blade protuberances.—The influence of protuberances on the blade is demonstrated in figures 4 to 7. It is seen from figure 3 that the fairings employed could not entirely eliminate the drag caused by the blade fittings, but the reduction in rotor drag due to the fairings amounted to about 15 pounds for

a 3,000-pound machine, or about 4 horsepower required at 100 miles per hour. Although it was necessary to obtain some information concerning the protuberance drag in order to evaluate the drag caused by the remainder of the rotor, the results are of minor practical importance because of the current trend toward the use of cantilever blades with no protuberances.

Effect of rotor speed and pitch angle.—Figures 8 to 10 illustrate the change in rotor characteristics with rotor speed and pitch setting. It is shown that at a constant pitch setting and tip-speed ratio there is a small but consistent increase of lift coefficient as the tunnel speed and rotor speed increase. The change in L/D is not absolutely consistent but appears to be an increase at low tip-speed ratios, culminating in a higher maximum and falling off more rapidly after the peak, as the rotor speed increases. The angle of attack also changes with rotor speed. Figure 8 shows a fairly consistent decrease in this quantity at a given tip-speed ratio as the rotor speed increases.

The effect of pitch setting on rotor characteristics may be ascertained by a comparison of figures 8, 9, and 10. At a given tip-speed ratio it is seen that the lift coefficient and L/D increase with the pitch setting, though there is a small difference between the L/D in figure 8 and in figure 10. The pitch setting does not change the tip-speed ratio at which maximum L/D occurs, this value of μ being approximately 0.35 for all blade settings.

By reference to the increase in rotor lift coefficient and change in L/D with rotor speed, it is found that the variations can be explained as a result of an increase in nominal pitch angle, caused in turn by the increase in thrust at greater rotor speeds. Evidence supporting this statement is afforded by the change in the positions of the envelopes of the C_L and L/D curves in figures 8, 9, and 10 corresponding to definite changes in the pitch setting, the variation of the same characteristics with rotor speed being closely parallel.

Vector sheaves.—The resultant force vectors of the rotor are projected upon the longitudinal and lateral planes containing the rotor axis in figures 11 to 13, each figure presenting average results for one pitch setting. The projections of the vectors in the longitudinal plane in each figure move forward with decreasing tip-speed ratio to a maximum distance from the axis at a tip-speed ratio of approximately 0.3. This type of variation is probably a consequence of the lag of the blade flapping behind the forces causing it, although present knowledge of the mechanics of the rotor is too meager to explain the center-of-pressure movement in detail.

The recession of the force vectors from the axis of rotation in a lateral direction as the tip-speed ratio increases can be reasonably interpreted. As the asymmetry of the rotor, represented by the tip-speed ratio, increases, the equalization of lift on opposite sides of

the plane of symmetry becomes more difficult and is less completely accomplished, causing a shift in the center of pressure almost proportional to the tip-speed ratio.

Velocity surveys.—The downwash-angle contours shown in figures 14 and 15 have several points of interest. There is an increase in downwash angle in passing from the leading to the trailing edge of the disk along the plane of symmetry, which is in agreement with the expected variation for a lifting surface of such large chord and low aspect ratio. The downwash also shows a peak occurring just aft of the transverse position of the retreating blade and a decreased downwash where the velocity over the retreating blade is reversed. These conditions are consistent with the large flapping motion, leading to high angles of attack, of the transverse retreating blade and the poor flow conditions in the reversed velocity region. Also noteworthy is the upflow in both forward quarters of the disk, near its edge.

The induced yaw angles plotted in figures 16 and 17 disclose little of interest. In figure 16 there is a pronounced yaw away from the plane of symmetry on the aft part of the disk, but this phenomenon is not exhibited on figure 17, made at a greater tip-speed ratio. No satisfactory explanation of this peculiar flow has been obtained.

CONCLUSIONS

1. The aerodynamic characteristics of the PCA-2 autogiro rotor change with rotor speed and/or thrust.
2. The existence of a blade twist proportional to thrust explains the change in rotor characteristics with thrust.

3. The maximum L/D of the rotor cannot be appreciably increased by increasing the pitch angle above approximately 4.5° at the blade tip.

4. The drag of protuberances on the rotor blade is an appreciable percentage of the total rotor drag, being more than 5 percent on the PCA-2 blades.

5. Lateral and longitudinal center-of-pressure travel is very small, being less than 2 inches in the plane of the rotor disk.

6. Pronounced variations in downwash exist at certain portions of the rotor disk.

LANGLEY MEMORIAL AERONAUTICAL LABORATORY,
NATIONAL ADVISORY COMMITTEE FOR AERONAUTICS,
LANGLEY FIELD, VA., October 12, 1934.

REFERENCES

1. Wheatley, John B.: Lift and Drag Characteristics and Gliding Performance of an Autogiro as Determined in Flight. T. R. No. 434, N. A. C. A., 1932.
2. Wheatley, John B.: Wing Pressure Distribution and Rotor-Blade Motion of an Autogiro as Determined in Flight. T. R. No. 475, N. A. C. A., 1933.
3. Wheatley, John B.: An Aerodynamic Analysis of the Autogiro Rotor with a Comparison between Calculated and Experimental Results. T. R. No. 487, N. A. C. A., 1934.
4. DeFrance, Smith J.: The N. A. C. A. Full-Scale Wind Tunnel. T. R. No. 459, N. A. C. A., 1933.
5. Silverstein, Abe: Scale Effect on Clark Y Airfoil Characteristics from N. A. C. A. Full-Scale Wind-Tunnel Tests. T. R. No. 502, N. A. C. A., 1934.
6. Theodoresen, Theodore, and Silverstein, Abe: Experimental Verification of the Theory of Wind-Tunnel Boundary Interference. T. R. No. 478, N. A. C. A., 1934.

TABLE I.—PITCH SETTING=1.9°, PROTUBERANCES EXPOSED

μ Tip- speed ratio	α Angle of attack	C_L Lift coeff- cient	C_D Drag coeff- cient	L/D Lift- drag ratio	N Rotor speed r.p.m.	C_l Rolling- moment coefficient	C_m Pitching- moment coefficient	C_y Lateral- force coeff- cient
0.133	18.7	0.605	0.228	2.65	98.3	0.001574	0.000130	0.0131
0.134	18.0	0.597	0.226	2.64	97.5	0.001242	0.000130	0.0130
0.139	13.3	0.423	0.115	3.68	98.8	0.001287	0.000192	0.0102
0.136	18.6	0.601	0.223	2.69	109.2	0.001845	0.000208	0.0077
0.148	16.1	0.540	0.176	3.07	119.7	0.002695	0.000756	0.0036
0.148	16.0	0.547	0.177	3.05	119.2	0.001653	0.000272	0.0036
0.210	9.0	0.277	0.0569	4.95	98.3	0.000931	0.000117	0.0061
0.210	9.0	0.278	0.0569	4.89	99.6	0.000639	0.000174	0.0061
0.182	11.1	0.373	0.0868	4.31	118.9	0.001001	0.000150	0.0064
0.182	11.5	0.376	0.0868	4.33	133.5	0.001074	0.000174	0.0064
0.188	18.5	0.614	0.213	2.87	133.9	0.001594	0.000315	0.0076
0.188	18.5	0.612	0.213	2.87	100.0	0.000715	0.000085	0.0047
0.237	7.5	0.217	0.0391	5.57	100.0	0.000717	0.000070	0.0047
0.274	5.7	0.150	0.0257	6.19	98.8	0.000414	0.000070	0.0041
0.275	5.7	0.159	0.0257	6.19	98.8	0.000752	0.000075	0.0031
0.216	8.3	0.271	0.0530	5.11	117.6	0.000846	0.000116	0.0062
0.217	8.4	0.269	0.0524	5.13	117.1	0.000846	0.000114	0.0062
0.161	14.1	0.409	0.136	3.67	137.6	0.001598	0.000271	0.0047
0.161	14.1	0.418	0.136	3.67	137.6	0.001057	0.000271	0.0044
0.206	9.0	0.318	0.0635	5.01	133.5	0.001057	0.000271	0.0044
0.207	8.8	0.335	0.0603	5.65	132.8	0.000941	0.000243	0.0043
0.171	12.8	0.466	0.1129	4.15	147.7	0.001300	0.000150	0.0073
0.170	12.8	0.469	0.1129	4.16	148.2	0.000986	0.000151	0.0077
0.245	6.7	0.207	0.0359	5.76	118.1	0.000560	0.000090	0.0068
0.246	6.8	0.198	0.0371	5.33	118.5	0.000316	0.000050	0.0068
0.309	4.8	0.123	0.0188	6.61	98.8	0.000316	0.000050	0.0062
0.207	4.8	0.123	0.0188	6.59	99.6	0.000236	0.000045	0.0062
0.278	5.4	0.160	0.0259	6.18	117.6	0.000565	0.000116	0.0065
0.224	7.8	0.268	0.0492	5.44	137.3	0.000580	0.000161	0.0041
0.225	7.8	0.266	0.0488	5.45	137.3	0.000832	0.000226	0.0041
0.199	9.6	0.351	0.0705	4.98	146.9	0.000721	0.000226	0.0050
0.201	9.7	0.349	0.0707	4.93	147.7	0.001174	0.000355	0.0017
0.341	4.0	0.0890	0.0140	7.07	98.0	0.000216	0.000048	0.0015
0.344	4.0	0.0890	0.0143	6.71	98.0	0.000216	0.000048	0.0015
0.372	3.5	0.0790	0.0120	6.58	98.0	0.000296	0.000070	0.0012
0.299	4.7	0.1350	0.0212	6.37	118.9	0.000386	0.000045	0.0028
0.310	4.7	0.1309	0.0204	6.42	118.1	0.000256	0.000047	0.0026
0.246	6.4	0.2185	0.0368	5.94	138.5	0.000439	0.000042	0.0029
0.249	6.5	0.215	0.0360	5.97	137.6	0.000492	0.000090	0.0027
0.226	7.8	0.279	0.0509	5.48	148.6	0.000698	0.000106	0.0044
0.224	7.8	0.279	0.0509	5.48	148.6	0.000282	0.000055	0.0025
0.312	4.4	0.1229	0.0190	6.47	118.5	0.000444	0.000072	0.0038
0.262	6.0	0.1924	0.0315	6.11	146.5	0.000744	0.000150	0.0011
0.286	7.0	0.250	0.0438	5.71	137.3	0.000744	0.000150	0.0011
0.386	3.4	0.0737	0.0160	6.70	119.7	0.000278	0.000036	0.0020
0.335	4.0	0.1050	0.0160	6.56	119.7	0.000512	0.000081	0.0033
0.278	5.3	0.165	0.0263	6.27	138.5	0.000512	0.000081	0.0033
0.257	6.1	0.207	0.0383	6.12	147.4	0.000585	0.000110	0.0035
0.414	3.0	0.0638	0.0104	8.05	97.5	0.000110	0.000009	0.0009
0.343	3.9	0.1004	0.0154	6.52	121.4	0.000448	0.000049	0.0020
0.292	4.8	0.1496	0.0226	6.37	138.5	0.000329	0.000075	0.0030
0.270	5.6	0.184	0.0289	6.37	146.1	0.000515	0.000075	0.0030
0.421	2.9	0.0624	0.0095	6.68	98.2	0.000258	0.000088	0.0009
0.308	4.5	0.1335	0.0200	6.65	138.5	0.000319	0.000046	0.0027
0.440	2.6	0.0534	0.0082	6.51	119.7	0.000317	0.000049	0.0015
0.382	3.3	0.0786	0.0124	6.59	136.8	0.000416	0.000062	0.0023
0.326	4.0	0.1177	0.0173	6.29	136.8	0.000416	0.000062	0.0023
0.412	2.4	0.0489	0.00777	6.52	117.1	0.000257	0.000050	0.0021
0.412	2.8	0.0652	0.0100	6.11	139.2	0.000377	0.000050	0.0021
0.318	3.18	0.1201	0.0144	6.29	147.4	0.000426	0.000097	0.0022
0.400	2.1	0.0444	0.00712	6.24	138.5	0.000448	0.000097	0.0022
0.414	2.9	0.0657	0.0101	6.50	121.4	0.000339	0.000027	0.0012
0.356	3.4	0.0855	0.0140	6.82	136.2	0.001337	0.000029	0.0018
0.329	3.8	0.1176	0.0174	6.75	148.2	0.000525	0.000032	0.0021
0.512	2.1	0.0390	0.00662	6.26	119.7	0.000259	0.000032	0.0004
0.443	2.7	0.0562	0.00897	6.59	137.3	0.000429	0.000047	0.0019
0.379	3.1	0.1013	0.0148	6.84	147.4	0.000268	0.000047	0.0019
0.352	3.5	0.0839	0.0125	6.82	138.5	0.000268	0.000047	0.0019
0.404	2.9	0.0871	0.0110	6.53	141.7	0.000348	0.000042	0.0014
0.405	2.9	0.0718	0.0110	6.70	152.3	0.000348	0.000042	0.0014
0.375	3.0	0.0885	0.0132	6.67	147.4	0.000553	0.000044	0.0015
0.584	1.9	0.0317	0.00562	5.66	99.7	0.000298	0.000033	0.0004
0.637	1.8	0.0403	0.00514	5.93	98.8	0.000298	0.000033	0.0004
0.517	2.1	0.0403	0.00514	5.93	120.5	0.000129	0.000018	0.0005
0.440	2.5	0.0588	0.00897	6.73	149.0	0.000278	0.000030	0.0010
0.412	2.7	0.0707	0.01050	6.73	149.0	0.000471	0.000030	0.0010
0.593	1.8	0.0305	0.00538	5.75	137.7	0.000099	0.000015	0.0003
0.493	2.1	0.0461	0.00749	6.23	137.7	0.000229	0.000022	0.0003
0.705	1.4	0.0240	0.00546	5.33	97.1	0.000149	0.000033	0.0001
0.608	1.6	0.0303	0.00546	5.61	120.5	0.000198	0.000034	0.0003
0.520	1.7	0.0418	0.00878	6.15	140.9	0.000287	0.000050	0.0005
0.722	1.2	0.0234	0.00459	5.09	102.1	0.000218	0.000023	0.0002

TABLE II.—PITCH SETTING=0.8°, PROTUBERANCES FAIRED

μ Tip- speed ratio	α Angle of attack	C_L Lift coeff- cient	C_D Drag coeff- cient	L/D Lift- drag ratio	N Rotor speed r.p.m.	C_l Rolling- moment coefficient	C_m Pitching- moment coefficient	C_y Lateral- force coeff- cient
0.124	19.7	0.509	0.199	2.56	111.3	0.001684	0.000174	0.0055
0.124	19.7	0.508	0.197	2.58	111.3	0.001348	0.000128	0.0058
0.125	19.6	0.519	0.199	2.61	124.6	0.001455	0.000066	0.0018

TABLE II.—PITCH SETTING=0.8°, PROTUBERANCES FAIRED—Continued

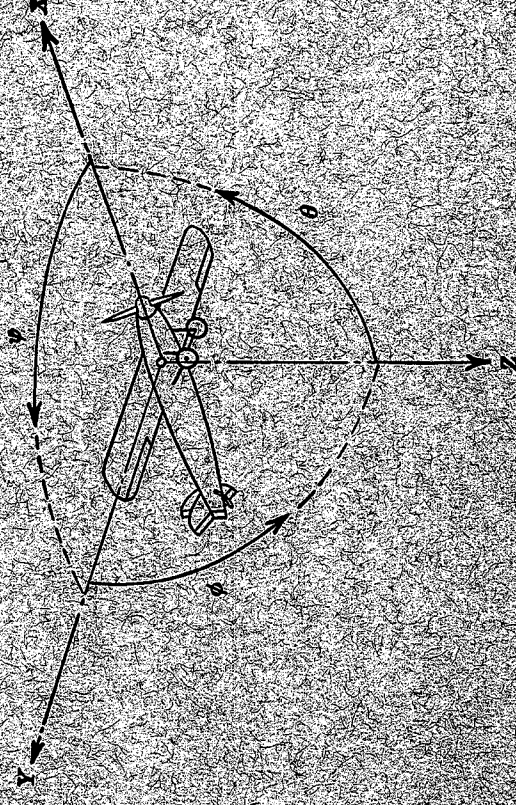
μ Tip- speed ratio	α Angle of attack	C_L Lift coeff- cient	C_D Drag coeff- cient	L/D Lift- drag ratio	N Rotor speed r.p.m.	C_l Rolling- moment coefficient	C_m Pitching- moment coefficient	C_y Lateral- force coeff- cient
0.125	19.6	0.515	0.198	2.60	124.3	0.001088	0.000156	0.0015
0.136	17.3	0.460	0.155	2.97	119.7	0.001500	0.000228	0.0034
0.136	17.3	0.456	0.155	2.94	120.0	0.001300	0.000385	0.0031
0.126	19.1	0.559	0.187	2.99	151.5	0.001516	0.000015	0.0029
0.126	19.1	0.558	0.188	2.97	151.5	0.001386	0.000009	0.0027
0.127	19.0	0.535	0.190	2.83	139.1	0.001875	0.000299	0.0007
0.127	19.0	0.535	0.190	2.81	138.9	0.001742	0.000154	0.0007
0.170	12.7	0.312	0.0808	3.86	121.0	0.001196	0.000164	0.0033
0.159	13.9	0.371	0.102	3.64	136.8	0.000869	0.000056	0.0009
0.157	13.8	0.378	0.103	3.67	136.8	0.000920	0.000121	0.0008
0.126	19.1	0.561	0.189	2.98	151.5	0.001529	0.000203	0.0024
0.126	19.1	0.561	0.189	2.97	151.5	0.000853	0.000132	0.0031
0.199	10.4	0.234	0.0526	4.45	119.2	0.000563	0.000062	0.0030
0.197	10.4	0.235	0.0526	4.47	119.2	0.000487	0.000117	0.0021
0.224	8.8	0.185	0.0373	4.96	118.9	0.000394	0.000079	0.0023
0.226	8.8	0.183	0.0369	4.96	119.2	0.000512	0.000057	0.0015
0.186	11.0	0.278	0.0636	4.37	136.8	0.000512	0.000057	0.0015
0.144	15.7	0.459	0.127	3.61	136.8	0.000359	0.000068	0.0029
0.143	15.7	0.463	0.129	3.59	137.2	0.001089	0.000078	0.0008
0.172	12.1	0.341	0.0784	4.35	138.0	0.001137	0.000277	0.0016
0.171	12.1	0.348	0.0792	4.40	138.4	0.000813	0.000277	0.0016
0.208	9.4	0.228	0.0465	4.90	140.4	0.001001	0.000281	0.0011
0.207	9.4	0.228	0.0465	4.90	140.4	0.000527	0.000294	0.0012
0.254	7.4	0.1429	0.0262	5.46	119.2	0.000254	0.000058	0.0016
0.255	7.4	0.1412	0.0259	5.46	119.2	0.000242	0.000058	0.0016
0.251	6.5	0.1156	0.0201	5.74	119.2	0.000242	0.000058	0.0016
0.281	6.5	0.1138	0.0198	5.74	118.9	0.000239	0.000052	0.0009
0.281	7.8	0.1677	0.0309					

TABLE III.—PITCH SETTING=1.9°, PROTUBERANCES FAIRED

μ Tip- speed ratio	α Angle of attack	C_L Lift coeff- cient	C_D Drag coeff- cient	L/D Lift- drag ratio	N Rotor speed r.p.m.	C_i Rolling- moment coefficient	C_m Pitching- moment coefficient	C_y Lateral- force coeff- cient
0.145	9	0.526	0.168	3.13	98.8	0.001319	0.000207	0.0136
.145	15.8	.535	.171	3.12	98.3	.001100	.000086	.0137
.132	18.4	.617	.227	2.72	102.1	.001231	.000077	.0133
.133	18.5	.617	.227	2.62	101.3	.001033	.000070	.0130
.181	11.2	.360	.0847	4.25	98.3	.0005311	.000085	.0083
.183	11.2	.368	.0866	4.24	99.2	.0008855	.000139	.0084
.133	18.4	.624	.228	2.73	114.7	.001395	.000042	.0066
.133	18.4	.624	.228	2.73	114.3	.001367	.000099	.0072
.153	14.6	.515	.151	3.42	121.4	.001130	.000263	.0059
.216	8.3	.258	.0491	5.26	100.5	.000841	.000171	.0057
.215	8.3	.259	.0493	5.26	100.5	.000660	.000127	.0057
.195	9.7	.330	.0700	4.72	117.1	.000936	.000405	.0075
.140	17.2	.613	.198	3.13	136.0	.001258	.000040	.0052
.249	6.6	.632	.0323	5.21	98.8	.000422	.000169	.0040
.222	7.7	.257	.0474	5.91	118.1	.000654	.000201	.0059
.171	12.2	.450	.111	4.05	137.2	.001951	.000829	.0038
.147	16.1	.586	.171	3.43	145.7	.001021	.000072	.0083
.275	5.5	.158	.0246	6.42	100.0	.000270	.000440	.0030
.252	6.1	.195	.0323	6.03	119.2	.000285	.000409	.0043
.207	8.7	.313	.0601	5.21	136.0	.000737	.000273	.0050
.182	11.0	.414	.0927	4.47	146.1	.001107	.000134	.0055
.315	4.3	1.161	.0170	6.83	98.8	.000980	.000248	.0009
.229	5.0	1.522	.0237	6.42	117.6	.001084	.000228	.0021
.205	7.1	.357	.0443	5.80	138.4	.001229	.000118	.0035
.301	3.7	.0965	.0141	6.84	147.7	.001045	.000195	.0005
.305	4.2	1.200	.0193	5.16	147.7	.001045	.000195	.0005
.252	5.8	.201	.0318	6.32	118.9	.000927	.000181	.0019
.232	6.9	.254	.0437	5.81	146.9	.001320	.000171	.0031
.373	3.2	.0736	.0116	6.86	98.8	.000884	.000012	.0004
.232	4.2	1.294	.0193	6.71	118.9	.000926	.000056	.0026
.231	6.9	.255	.0435	5.86	146.5	.001076	.000068	.0040
.369	3.2	.0828	.0151	7.13	98.8	.000884	.000011	.0040
.268	5.4	1.179	.0282	6.44	136.8	.000612	.000045	.0012
.324	4.0	1.103	.0164	6.73	117.6	.000612	.000045	.0012
.242	6.3	.233	.0378	6.10	145.7	.000989	.000038	.0036
.394	3.0	.0697	.0100	6.97	98.0	.000029	.000014	.0010
.288	4.7	.150	.0227	6.87	122.6	.000348	.000042	.0021
.331	3.7	.0872	.0156	6.61	137.2	.000443	.000064	.0029
.260	5.5	.200	.0311	6.43	148.2	.000336	.000050	.0034
.418	2.7	.0616	.0090	6.85	98.3	.000039	.000017	.0008
.356	3.4	.0897	.0132	6.79	118.9	.000098	.000006	.0011
.300	4.3	1.382	.0294	6.80	137.7	.000096	.000040	.0028
.274	5.0	.176	.0268	6.56	146.9	.000426	.000058	.0031
.361	2.6	.0673	.0085	6.75	99.2	.000186	.000059	.0017
.369	3.2	.0828	.0151	6.96	120.0	.000107	.000035	.0025
.314	3.9	1.251	.0181	6.91	138.5	.000404	.000038	.0028
.289	4.4	.155	.0225	6.86	145.7	.000358	.000013	.0028
.452	2.4	.0513	.00794	7.02	99.6	.000059	.000020	.0006
.382	2.8	.0768	.0108	6.46	120.5	.000127	.000037	.0016
.325	3.6	1.160	.0166	6.99	138.9	.000405	.000074	.0023
.303	3.9	.1397	.0199	7.01	147.3	.000360	.000023	.0026
.467	2.2	.0476	.0070	6.43	100.0	.000025	.000007	.0006
.345	2.5	.1005	.0143	6.92	118.1	.000129	.000030	.0009
.319	3.7	.1239	.0178	6.96	149.9	.000069	.000049	.0020
.496	1.9	.0421	.0065	6.47	99.2	.0000485	.000029	.0005
.438	2.3	.0560	.0083	6.75	117.2	.000148	.000028	.0008
.355	3.0	.0961	.0137	7.01	141.7	.000418	.000047	.0019
.337	3.4	.0373	.00601	6.32	98.0	.000297	.000006	.0004
.526	1.9	.0373	.00601	6.32	98.0	.000043	.000006	.0004
.417	2.2	.0505	.00764	6.65	117.2	.000092	.000018	.0007
.381	2.7	.0805	.0115	7.00	139.2	.000269	.000020	.0016
.351	3.0	.0999	.0140	7.13	147.7	.000258	.000043	.0018
.552	1.7	.0336	.00549	6.22	97.6	.000086	.000005	.0003
.406	2.0	.0430	.00684	6.42	118.1	.000180	.000025	.0006
.389	2.6	.0647	.00957	6.81	138.7	.000097	.000014	.0012
.591	1.7	.0300	.00521	5.77	100.0	.000150	.000025	.0003
.528	2.1	.0378	.00621	6.10	119.2	.000239	.000025	.0005
.458	2.3	.0528	.00790	6.77	136.4	.000200	.000025	.0008
.645	1.6	.0257	.00534	5.81	140.9	.000290	.000044	.0011
.588	1.5	.0311	.00534	5.71	98.0	.000009	.000003	.0001
.491	1.3	.0450	.00725	5.87	116.7	.000250	.000025	.0004
.701	1.3	.0233	.00431	5.42	138.5	.000348	.000051	.0007
.623	1.3	.0287	.00511	5.74	118.1	.000110	.000032	.0001
.525	1.6	.0394	.00649	5.06	140.0	.000230	.000027	.0004
.724	1.1	.0223	.00425	5.55	102.1	.000028	.000032	.0001

TABLE IV.—PITCH SETTING=2.7°, PROTUBERANCES FAIRED

μ Tip- speed ratio	α Angle of attack	C_L Lift coeff- cient	C_D Drag coeff- cient	L/D Lift- drag ratio	N Rotor speed r.p.m.	C_i Rolling- moment coefficient	C_m Pitching- moment coefficient	C_y Lateral- force coeff- cient
0.145	16.9	0.670	0.2108	3.18	117.2	0.002270	0.000649	0.0093
.145	16.9	.670	.2108	3.18	117.2	.002051	.000720	.0088
.170	12.7	.597	.1310	3.97	119.7	.001522	.000370	.0073
.170	12.7	.597	.1310	3.87	119.7	.001296	.000208	.0067
.143	17.9	.689	.2148	3.18	127.0	.001647	.000389	.0136
.143	17.9	.689	.2148	3.18	127.0	.001441	.000191	.0137
.174	15.4	.592	.1225	4.81	128.9	.001215	.000279	.0086
.174	15.4	.592	.1225	4.81	128.9	.001155	.000324	.0086
.203	8.0	.386	.0768	4.65	120.9	.001458	.000355	.0053
.202	8.0	.386	.0768	4.65	120.9	.001370	.000443	.0053
.215	8.3	.359	.0676	5.29	128.1	.000870	.000143	.0062
.215	8.3	.359	.0676	5.29	128.1	.000832	.000221	.0057
.242	6.3	.266	.0439	6.01	116.2	.000719	.000178	.0046
.242	6.3	.266	.0439	6.01	116.2	.000699	.000248	.0046
.242	6.4	.271	.0455	6.04	120.5	.001022	.000176	.0049
.240	6.4	.271	.0455	6.04	120.5	.000980	.000177	.0049
.270	4.8	.206	.0309	6.68	116.2	.000472	.000384	.0037
.270	4.8	.206	.0309	6.68	116.2	.000466	.000384	.0037
.268	5.0	.216	.0326	6.62	126.3	.000652	.000116	.0042
.268	5.0	.216	.0326	6.62	126.3	.000610	.000117	.0042
.297	3.9	.167	.0241	6.93	119.0	.000475	.000070	.0036
.294	4.3	.187	.0274	6.93	119.0	.000361	.000109	.0034
.285	4.3	.185	.0275	6.73	128.4	.000471	.000096	.0035
.308	3.6	.151	.0215	7.02	119.7	.000442	.000104	.0033
.305	3.6	.154	.0217	7.10	120.5	.000350	.000099	.0033
.305	3.6	.154	.0217	7.10	120.5	.000349	.000099	.0033
.335	3.0	.107	.0225	6.98	128.9	.000462	.000169	.0033
.330	3.0	.1231	.0176	7.06	119.2	.000550	.000116	.0033
.315	3.4	.1479	.0207	7.02	127.5	.000316	.000046	.0029
.315	3.4	.1479	.0207	7.02	127.5	.000345	.000071	.0028
.349	2.7	.1148	.0162	7.09	118.9	.000347	.000062	.0028
.350	2.7	.1147	.0161	7.11	118.9	.000308	.000053	.0028
.334	3.3	.1303	.0182	7.16	129.5	.000455	.000076	.0028
.368	2.4	.1030	.0144	7.13	119.0	.000210	.000117	.0031
.368	2.4	.1030	.0144	7.13	119.0	.000207	.000148	.0024
.356	2.5	.1195	.0156	7.21	128.8	.000387	.000051	.0026
.353	2.5	.1169	.0158	7.21	128.8	.000270	.000029	.0026
.390	2.0	.0874	.0124	7.08	116.3	.000107	.000019	.0020
.396	2.0	.0867	.0121	7.08	116.3	.000084	.000019	.0020
.377	2.2	.1013	.0141	7.13	129.1	.000301	.000062	.0017
.374	2.2	.1013	.0141	7.13	129.1	.000310	.000062	.0017
.409	1.8	.0802	.0114	7.04	119.2	.000310	.000024	.0015
.412	1.8	.0800	.0125	7.19	119.2	.000339	.000024	.0015
.392	2.0	.0890	.0125	7.19	128.0	.000219	.000023	.0014
.392	2.0	.0890	.0125	7.19	128.0	.000240	.000023	.0014
.429	1.6	.0717	.0102	7.24	118.1	.000149	.000043	.0013
.429	1.6	.0717	.0102	7.24	118.1	.000230	.000032	.0016
.414	1.8	.0841	.0112	7.03	128.8	.000301	.000062	.0017
.409	1.8	.0841	.0112	7.11	129.1	.000351	.000061	.0011
.445	1.5	.0663	.00970	6.84	119.2	.000310	.000024	.0015
.446	1.5	.0663	.00970	6.84	119.2	.000339	.000024	.0015
.438	1.6	.0693	.00961	7.07	128.0	.000219	.000023	.0014
.434	1.6	.0707	.0103	7.07	128.0	.000248	.000023	.0014
.480	1.4	.0540	.00847	6.48	129.1	.000240	.000041	.0011
.481	1.4	.0540	.00847	6.48	129.1	.000351	.000041	.0011
.481	1.4	.0540	.00847	6.48	129.1	.000219	.000026	.0013
.449	1.6							



Positive directions of axes and angles (forces and moments) are shown by arrows

Axis		Forces (parallel to axis)		Moment about axis		Velocities	
Designation	Symbol	Designation	Symbol	Designation	Symbol	Designation	Symbol
Longitudinal	X	Rolling	L	Positive direction	Y → Z	Linear (component along axis)	u
Lateral	Y	Pitching	M		Z → X		v
Normal	Z	Yawing	N		X → Y	Angular	ω

Absolute coefficients of moment

$$C_l = \frac{L}{\rho b S} \quad \text{(rolling)}$$

$$C_m = \frac{M}{\rho b S} \quad \text{(pitching)}$$

$$C_n = \frac{N}{\rho b S} \quad \text{(yawing)}$$

Angle of set of control surface (relative to neutral position) δ . (Indicate surface by proper subscript.)

4. PROPELLER SYMBOLS

D , Diameter

p , Geometric pitch

p/D , Pitch ratio

V_i , Inflow velocity

V_s , Slipstream velocity

T , Thrust, absolute coefficient $C_T = \frac{T}{\rho n^3 D^4}$

Q , Torque, absolute coefficient $C_Q = \frac{Q}{\rho n^3 D^5}$

P , Power, absolute coefficient $C_P = \frac{P}{\rho n^3 D^5}$

C_s , Speed-power coefficient $= \sqrt[5]{\frac{P}{\rho n^3}}$

η , Efficiency

n , Revolutions per second, r.p.s.

ϕ , Effective helix angle $= \tan^{-1} \left(\frac{V}{2\pi r m} \right)$

5. NUMERICAL RELATIONS

1 hp. = 76.04 kg-m/s = 550 ft-lb./sec.

1 metric horsepower = 1.0132 hp.

1 m.p.h. = 0.4470 m.p.s.

1 m.p.s. = 2.2369 m.p.h.

1 lb. = 0.4536 kg.

1 kg = 2.2046 lb.

1 m. = 1.609.35 m = 5,280 ft.

1 m = 3.2808 ft.

NACA FILE COPY

Loan expires on last
date stamped on back cover.

PLEASE RETURN TO

**REPORT DISTRIBUTION AND STORAGE SECTION
LANGLEY AERONAUTICAL LABORATORY
NATIONAL ADVISORY COMMITTEE
FOR AERONAUTICS**

Langley Field, Virginia